Synthesis and Characterization of Cyclic Liquid Crystalline Oligomers Based on 1-(4-Hydroxy-4′-biphenylyl)-2-(4-hydroxyphenyl)butane and 1,10-Dibromodecane[1]

V. Percec* and M. Kawasumi

Department of Macromolecular Science, Case Western Reserve University, Cleveland, Ohio 44106

P. L. Rinaldi and V. E. Litman

Department of Chemistry, University of Akron, Akron, Ohio 44325

Received January 21, 1992; Revised Manuscript Received March 30, 1992

ABSTRACT: The synthesis of cyclic monomer, dimer, trimer, tetramer, and pentamer based on 1-(4-hydroxy-4′-biphenylyl)-2-(4-hydroxyphenyl)butane (TPB) and 1,10-dibromodecane and their characterization by 300-MHz 1-D ^{1}H-NMR and 2-D ^{1}H-NMR COSY and NOESY spectroscopies, differential scanning calorimetry, and optical polarized microscopy are presented. Their phase behavior was compared with that of the linear high molecular weight polymer based on TPB and 1,10-dibromodecane. The cyclic monomer is liquid. The larger cyclic compounds exhibit a nematic mesophase and a very slow crystallization tendency. Their melting temperature shows an odd–even dependence on ring size, while their isotropization transition temperature shows a continuous increase versus ring size. The cyclic tetramer and pentamer exhibit higher isotropization transition temperatures but lower enthalpy and entropy changes than the corresponding linear high molecular weight polymer. An explanation for this behavior is provided.

Introduction

Cyclic oligomers are generated during both step condensation and ring-opening polymerization reactions.[2] Therefore, unless removed they are available in many polymers synthesized by these synthetic methods. In addition, cyclic oligomers (i.e., ionophores)[3] and polymers (i.e., DNA and peptides)[2c] are important natural compounds. However, there is very little understanding of the differences and similarities between cyclic and linear oligomers and polymers. This is due to the lack of reliable preparative methods for their synthesis. Presently, cyclic glassy oligomers and polymers, i.e., polystyrene,[2a,b,4] polysiloxanes,[2,5] and poly(2-vinylpyridine)[6] have been synthesized and characterized. Cyclic oligomeric polycarbonate[7] and few other condensation polymers[8] have also been synthesized. Cyclic oligomers of polyethylene were synthesized and used to understand the crystallization mechanism of polyethylene.[2a,9] Cyclic side-chain liquid crystalline oligomers and polymers were recently reported.[10]

The goal of this paper is to describe the synthesis and characterization of the first examples of cyclic main-chain liquid crystalline polymers. In a previous series of publications from our laboratory we have advanced the concept of liquid crystalline polyethers based on conformational isomerism (Scheme I).[11-13] Mesogenic units based on conformational isomerism such as 1-(4-hydroxy-4′-biphenylyl)-2-(4-hydroxyphenyl)butane (TPB)[13] are ideal structures for the synthesis of cyclic main-chain liquid crystalline polymers since their gauche conformer favors the cyclization reaction (Scheme I). This paper reports the synthesis and characterization of cyclic polyethers based on TPB and 1,10-dibromodecane. All molecular receptors with at least one aromatic ring bridged by at least one aliphatic n-membered bridge ($n \geq 0$) may be called cyclophanes.[14] Therefore, the cyclic oligomers based on TPB and α,ω-dibromoalkanes reported in this paper represent the first examples of liquid crystalline cyclophanes.

Scheme I
Conformation Isomerism of TPB and Its Cyclization with 1,10-Dibromodecane under High-Dilution Conditions

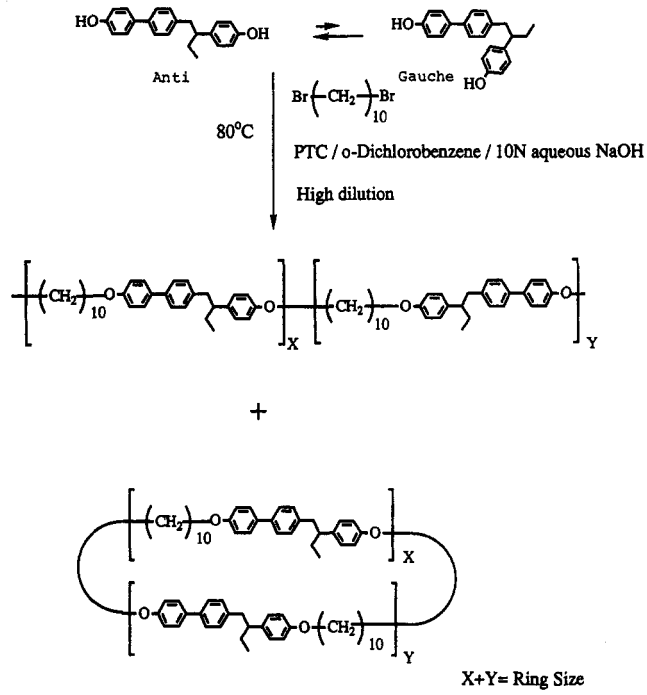

Experimental Section

Materials. Tetrabutylammonium hydrogen sulfate (TBAH) (97%; Aldrich) was used as received. 1,10-Dibromodecane (97%) (Aldrich) was purified by vacuum distillation. *o*-Dichlorobenzene was distilled under reduced pressure. 1-(4-Hydroxy-4′-biphenylyl)-2-(4-hydroxyphenyl)butane (TPB) (purity >99% by HPLC) was synthesized according to the previously described procedure.[13] Silica gel plates with fluorescent indicator (Eastman Kodak) were used for thin-layer chromatography (TLC) analyses. All other chemicals were commercially available and were used as received.

0024-9297/92/2225-3851$03.00/0

Polyetherification Experiments. The linear polyether with low molecular weight (M_n = 12 700 by GPC) was synthesized by a liquid–liquid two-phase (*o*-dichlorobenzene/NaOH aqueous solution, 10 times excess to the phenol groups) phase-transfer-catalyzed polyetherification of TPB with 1,10-dibromodecane according to the previously described procedure[13] except that the amount of 1,10-dibromodecane was 1.1 mol to 1.0 mol TPB instead of 1.0 to 1.0.

Phase-Transfer-Catalyzed Polymerization of TPB with 1,10-Dibromodecane. The polyetherifications of 1-(4-hydroxy-4′-biphenylyl)-2-(4-hydroxyphenyl)butane with 1,10-dibromodecane were carried out at various concentrations [monomer (mmol)/organic solvent (mL) = 1/2, 1/20, and 1/100] under a nitrogen atmosphere at 80 °C in an *o*-dichlorobenzene–10 N NaOH aqueous solution mixture in the presence of tetrabutylammonium hydrogen sulfate as phase-transfer catalyst. Samples of the reaction mixture were collected at various reaction times and analyzed by gel permeation chromatography. The procedure used in all polyetherifications is as follows.

Experiment 1 [Monomer (mmol)/Solvent (mL) = 1/2]. To a 25-mL single-neck flask equipped with a condenser were added successively 0.318 g (1.00 mmol) of TPB, 2.0 mL of 10 N NaOH aqueous solution (20 mmol), 2.0 mL of *o*-dichlorobenzene, 0.300 g (1.00 mmol) of 1,10-dibromodecane, and 0.136 g (0.40 mmol, 20 mol % of phenol groups) of TBAH. A balloon filled with nitrogen was placed at the top of the condenser. The reaction mixture was stirred at 1100 rpm with a magnetic stirrer at 80 °C. After 15 min, 30 min, 45 min, 1 h, 2 h, 4 h, and 6 h, a part of the reaction mixture was collected. Each reaction mixture was diluted with water and chloroform, and the aqueous layer was removed. The organic layer was washed with water, then with dilute hydrochloric acid, and again three times with water. The solvents were evaporated on a rotary evaporator to give the polyether as a solid. The obtained polyether was precipitated in water from THF solution two times to remove completely the inorganic salt. After it was dried in vacuo, the product was analyzed by gel permeation chromatography.

Experiment 2 [Monomer (mmol)/Solvent (mL) = 1/20]. The procedure was the same as that used in experiment 1 except that a 100-mL single-neck flask was used. The amounts of 10 N NaOH aqueous solution (200 mmol) and *o*-dichlorobenzene were 20 mL each. The sampling times were 1, 2, 3, 4, 6, 8, and 10 h.

Experiment 3 [Monomer (mmol)/Solvent (mL) = 1/100]. The procedure was the same as that used in experiment 1 except that a 500-mL single-neck flask was used. The amounts of 10 N NaOH aqueous solution (1.0 mol) and *o*-dichlorobenzene were both 100 mL. The sampling times were 1, 3, 6, 9, 12, 24, and 72 h. After the dilution of the reaction mixture with water and chloroform, the aqueous layer was separated in a separatory funnel. The organic layer was washed with water, then with dilute hydrochloric acid, and again six times with water. The solvents were evaporated on a rotary evaporator to give a solid product containing a liquid product. The products were analyzed directly by gel permeation chromatography without precipitation.

Experiment 4. Preparation of Cyclic Oligomers. The polyetherification of 1-(4-hydroxy-4′-biphenylyl)-2-(4-hydroxyphenyl)butane with 1,10-dibromodecane was carried out under high-dilution conditions [monomer (mmol)/solvent (mL) = 1/100] under a nitrogen atmosphere at 80 °C in an *o*-dichlorobenzene–10 N NaOH aqueous solution in the presence of TBAH as phase-transfer catalyst. Then the reaction mixture was separated into cyclic oligomers and a higher molecular weight part. The procedure for the preparation of cyclic polyethers is as follows.

To a 500-mL single-neck flask equipped with a condenser were successively added 0.318 g (1.00 mmol) of TPB, 100 mL of 10 N NaOH aqueous solution (1.0 mol), 100 mL of *o*-dichlorobenzene, 0.300 g (1.00 mmol) of 1,10-dibromodecane, and 0.136 g (0.40 mmol, 20 mol % of phenol groups) of TBAH. A balloon filled with nitrogen was placed at the top of the condenser. The reaction mixture was stirred at 1100 rpm with a magnetic stirrer at 80 °C. After 40 h, the reaction mixture was diluted with water and chloroform. The organic layer was washed two times with water, with dilute hydrochloric acid, and three times with water. After the evaporation of the solvents, the product was dissolved in chloroform. To this solution silica gel was added and the chloroform was evaporated. The product absorbed on silica gel was charged on the top of a column containing silica gel and was flushed with acetone to separate the mixture of cyclic oligomers. The remaining product at the top of the column was flushed with chloroform to separate the higher molecular weight part. The mixture of cyclic oligomers was separated into about 50 fractions by silica gel column chromatography with a mixture of acetone and hexanes (1:20 v/v). Each fraction was checked by TLC [developed by a mixture of acetone and hexanes (1:15 to 1:20 v/v) and detected with a UV lamp]. The fraction containing each cyclic was collected, and the solvents were evaporated on a rotary evaporator to give the separated cyclic oligomer. The cyclic dimer and trimer were further purified by recrystallization from hexanes.

Techniques. 1-D and 2-D ^{1}H-NMR (300 MHz) spectra were recorded on a VXR 300 NMR spectrometer at 299.949 MHz using a 5-mm ^{1}H–^{19}F broad-band switchable probe. Data were collected at ambient temperature without sample spinning. COSY spectra were acquired with 8 sets of pulses at the beginning of the experiment to establish a steady state. A total of 512 fid's were acquired with 16 transients, a 20.8-μs 90° pulse width, a 0.189–0.407 acquisition time (1024–2048 data points), a 1-s relaxation delay, and a 2715.9-Hz spectrum window in *f*1 and *f*2. The COSY spectra were processed with floating-point transforms, zero filling to 2048 or 4096 in *t*2 and 1024 in *t*1, and sine bell weighting. Phase-sensitive 2-D NOESY spectra were collected at ambient temperature without sample spinning. At the beginning of the experiment 8 dummy fid's were collected to establish a steady state. A total of 512 fid's were acquired with 16 transients, a 20.8-μs 90° pulse width, a 0.377–0.407 acquisition time (2048 data points), a 1-s relaxation delay, and a 2647.6-Hz spectral window in *f*1 and *f*2. A mixing time of 2 s was used. The NOESY spectra were processed with floating-point transforms.

Relative molecular weights and purities were determined by gel permeation chromatography (GPC) and high-pressure liquid chromatography (HPLC). GPC analyses were carried out with a Perkin-Elmer series 10 LC equipped with an LC-100 column oven, and a Nelson Analytical 900 series data station. The measurements were made by using the UV detector, chloroform as solvent (1 mL/min, 40 °C), two PL gel columns of 5×10^2 and 10^4 Å, and a calibration plot constructed with polystyrene standards. HPLC analyses were performed with the same instrument with a PL gel column of 1×10^2 Å.

A Perkin-Elmer DSC-4 differential scanning calorimeter equipped with a TADS data station Model 3600 was used to determine the thermal transitions. Heating and cooling rates were 20 °C/min in all cases. First-order transitions (crystalline–crystalline, crystalline–liquid crystalline, liquid crystalline–isotropic, etc.) were read at the maximum or minimum of the endothermic or exothermic peaks. Glass transition temperatures (T_g) were read at the middle of the change in the heat capacity. All heating and cooling scans after the first heating scan produced perfectly reproducible data. We will report the transitions collected from first and second or subsequent heating scans and from first cooling scan.

A Carl Zeiss optical polarizing microscope (magnification 100×) equipped with a Mettler FP 82 hot stage and a Mettler FP 800 central processor was used to observe the thermal transitions and to analyze the anisotropic textures.[15]

Molecular modeling and energy minimization experiments were carried out with ALCHEMY II software (Tripos Associates) on a Macintosh IIci personal computer.

Results and Discussion

Linear Polyetherification versus Cyclization and Separation of Cyclic Oligomers. Scheme I presents the polyetherification of TPB with 1,10-dibromodecane. TPB is a mesogenic unit based on conformational isomerism. Its gauche conformer should prefer intramolecular cyclization to intermolecular extension.

Figure 1 presents the GPC chromatograms versus reaction time obtained from experiments 1–3. M_n and M_w versus time are plotted in Figure 2. The rate of polyetherification at monomer (mmol)/solvent (mL) = 1/2 was

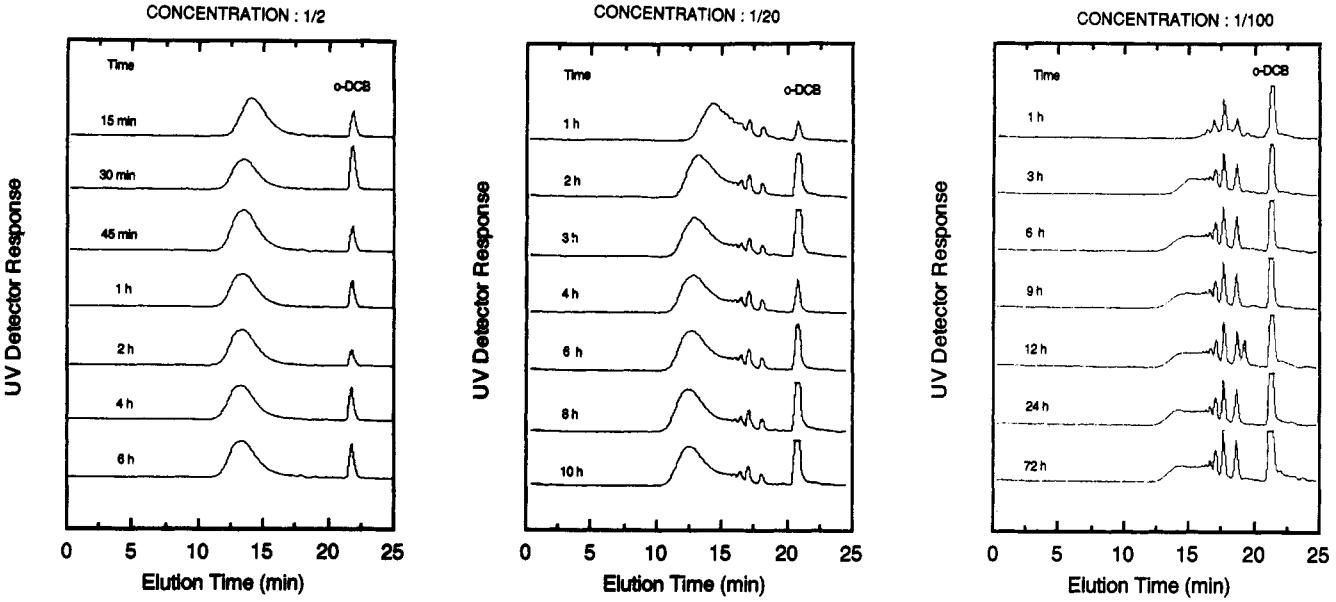

Figure 1. GPC chromatograms of the polymerization mixtures obtained at various reaction times and initial monomer concentrations: (a, left) monomer (mmol)/solvent (mL) = 1/2 (experiment 1); (b, middle) monomer (mmol)/solvent (mL) = 1/20 (experiment 2); (c, right) monomer (mmol)/solvent (mL) = 1/100 (experiment 3).

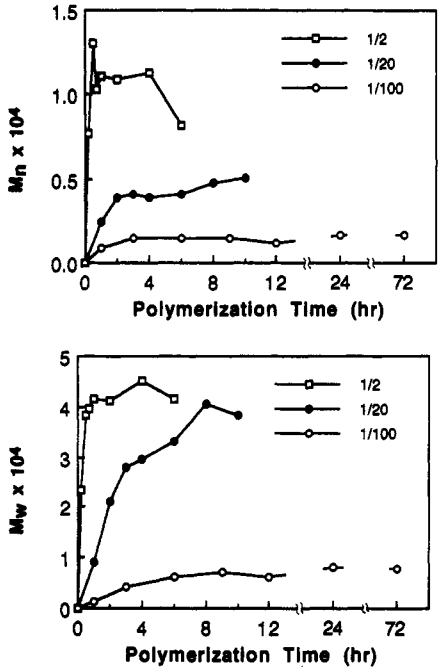

Figure 2. Dependence of the average molecular weights on the polymerization time at various initial monomer concentrations [monomer (mmol)/solvent (mL) = 1/2, 1/20, and 1/100]; (a, top) number-average molecular weight (M_n); (b, bottom) weight-average molecular weight (M_w).

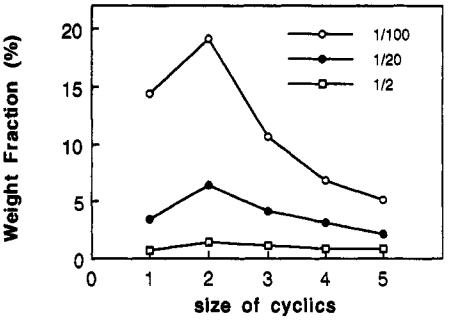

Figure 3. Weight fraction of cyclic oligmers versus the ring size obtained at various initial monomer concentrations [monomer (mmol)/solvent (mL) = 1/2, 1/20, and 1/100].

very fast. M_n and M_w became independent of the reaction time after 30 min. A very small amount of cyclic oligomers was formed at this concentration. The rate of polymerization at monomer (mmol)/solvent (mL) = 1/20 was slower than that at monomer (mmol)/solvent (mL) = 1/2. However, the molecular weight of the polymer reached the same level as that obtained in experiment 1 after 8 h. The maximum M_n was lower than that at monomer (mmol)/solvent (mL) = 1/2. The cyclic oligomers were formed at the beginning of the polymerization, and the amount and the ratio of different cyclics did not change during the polymerization. This can be explained by the irreversibility of each etherification step. As the concentration of monomer in the reaction mixture was decreased to monomer (mmol)/solvent (mL) = 1/50, the content of cyclic oligomers increased even more. The highest molecular weight of the polymer did not reach the same level as that obtained at monomer (mmol)/solvent (mL) = 1/2.

Figure 3 presents the dependence of the weight fraction of cyclic oligomers versus the ring size of cyclics. The weight fraction of cyclics increases with decreasing concentration of the monomer in the reaction mixture. This is due to the different dependence of intramolecular cyclization versus intermolecular reaction on monomer concentration. The intramolecular cyclization involves only a single molecule, and, therefore, it is a first-order reaction on the concentration of the growing chain. On the other hand, the intermolecular reaction which leads to linear extension is a second-order reaction in the concentration of the growing chain. Therefore, the intramolecular cyclization becomes more favorable than the linear polymerization with decreasing monomer concentration. The cyclic dimer is the dominant species regardless of the extent of the dilution. As the cyclic oligomer becomes larger, its weight fraction tends to decrease. This can be explained based on a kinetics effect as follows. If the chain becomes longer, it is less probable for both chain ends of one molecule to encounter and react with each other. However, this is not the case of the cyclic monomer. This may be due to the unfavorable strained conformation of the cyclic monomer, which will be discussed in the section on NMR spectroscopy. TPB has a chiral center[13] and, therefore, since we use the racemic mixture of its two enantiomers, upon polymerization with 1,10-dibromodecane we generate cyclic copolymers which from tetramer

Table I
Characterization of Cyclic Oligomers and Corresponding Linear Polymers

ring size	yield (%)	purity by HPLC	MW by GPC at the peak top measd	MW by GPC at the peak top calcd	thermal transitions (°C) and corresponding enthalpy changes (kcal/mru) in parentheses[a] heating	cooling
1	2.4	99	542	457	g <-10 i	i <-10 g
2	3.6	92	1154	913	g 53 k 90 k 113 (5.78[b]) i g 23 n 46 (0.15) i	i 41 (0.08) n 17 g
3	1.6	95	1845	1370	g 37 k 63 (1.19) n 95 (0.27) i g 28 n 94 (0.32) i	i 87 (0.32) n 20 g
4	2.3	96	2343	1827	g 50 k 55 k 82 k 121 n 130 (3.13[b]) i g 29 n 127 (1.21) i	i 124 (1.18) n 25 g
5	0.8	c	3100	2283	g 36 k 45 (0.09) n 127 (1.21) i g 33 n 128 (1.14) i	i 123 (1.19) n 26 g
$CHCl_3$-eluted part			M_n = 11 800, M_w/M_n = 1.53		g 49 k 57 k 71 n 97 (2.69[b]) i g 28 n 98 (2.31) i	i 89 (2.45) n 24 g
linear			M_n = 12 700, M_w/M_n = 1.48		g 44 k 62 (0.97) n 103 (1.83) i g 31 n 103 (1.94) i	i 93 (1.94) n 25 g
linear			M_n = 37 700, M_w/M_n = 2.22		g 42 k 48 (0.03) n 112 (2.54) i g 43 n 112 (2.54) i	i 96 (2.61) n 35 g

[a] Data on the first line are from first heating and cooling scans. Data on the second line are from second heating scan. [b] Overlapped peaks. [c] It contains trimer, tetramer, and higher cyclics. However, each cyclic is overlapped severely and purity could not be determined.

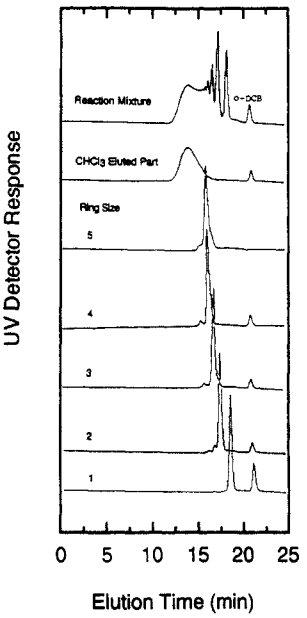

Figure 4. GPC chromatograms of the polymerization mixture, of the part eluted with $CHCl_3$, and of the separated cyclic oligomers obtained from experiment 4.

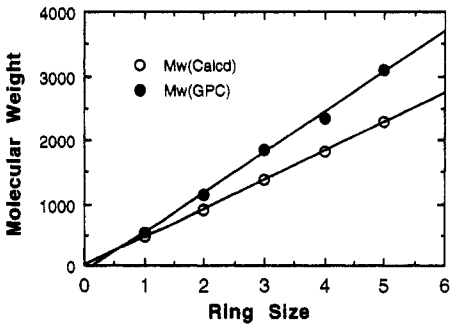

Figure 5. Peak molecular weight of cyclic oligomers obtained by GPC versus the ring size.

on contain all four constitutional isomers of TPB. The lower cyclics contain three (trimer), two (dimer) and one (monomer) isomers. Therefore, the cyclic oligomers lower than the tetramer are mixtures of compounds based on various isomers.

Figure 4 shows the GPC chromatograms of the reaction mixture, of the high molecular weight part eluted with chloroform, and of the individual cyclic oligomers obtained

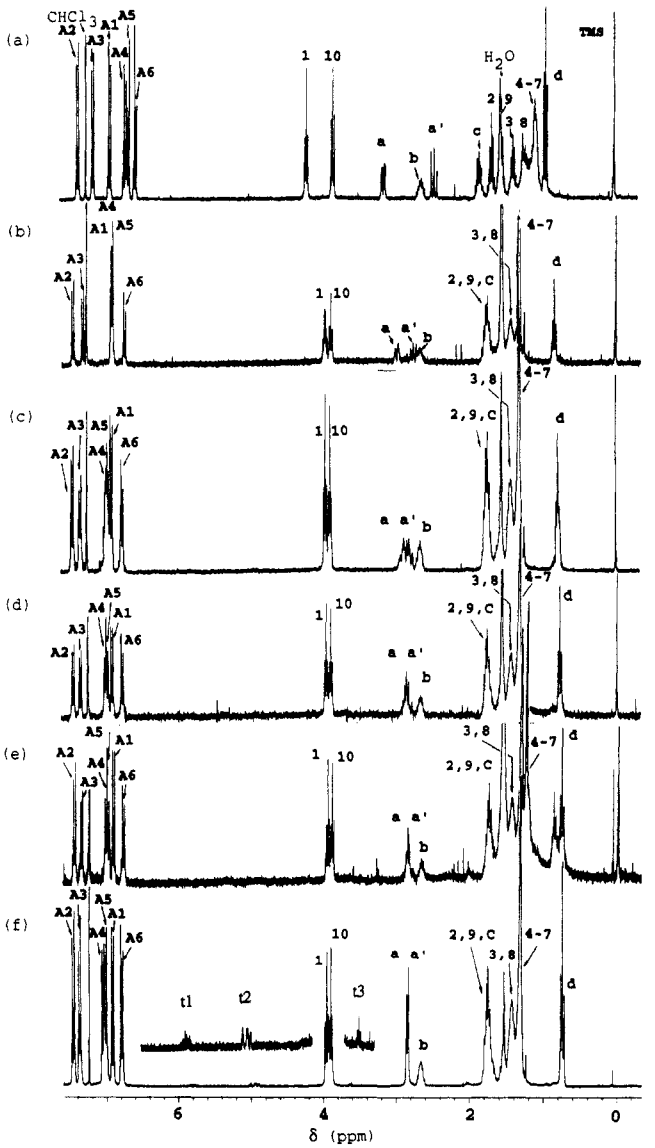

Figure 6. 300-MHz ^{1}H-NMR spectra of cyclic monomer (a), cyclic dimer (b), cyclic trimer (c), cyclic tetramer (d), crude cyclic pentamer (e), $CHCl_3$-eluted part (f) and linear polyether (M_n = 12 700) ($CDCl_3$, TMS).

in experiment 4. The purity and molecular weight at the peak top of each cyclic are presented in Table I. The purity of the cyclic oligomers is >92% except for the case

Table II
^{1}H-NMR Peak Assignments of Cyclic Oligomers, of the $CHCl_3$-Eluted Part, and of Linear Polyether

	peak assignments (ppm)																				
ring size	A1	A2	A3	A4	A5	A6	a	a′	b	c	d	1	2	3	4	5	6	7	8	9	10
1	6.91	7.36	7.14	6.68	6.64	6.54	3.13	2.44	2.62	1.83	0.92	4.18	1.66	1.37	1.07	1.07	1.07	1.07	1.24	1.54	3.82
2	6.90	7.43	7.29	6.88	6.87	6.72	2.95	2.74	2.66	1.75	0.82	3.97	1.75	1.43	1.30	1.30	1.30	1.30	1.43	1.75	3.87
3	6.90	7.44	7.33	6.99	6.93	6.75	2.87	2.80	2.63	1.76	0.77	3.95	1.76	1.44	1.30	1.30	1.30	1.30	1.44	1.76	3.89
4	6.90	7.44	7.34	7.01	6.96	6.76	2.83	2.83	2.66	1.73	0.75	3.95	1.73	1.41	1.30	1.30	1.30	1.30	1.41	1.73	3.87
5	6.90	7.44	7.35	7.01	6.98	6.76	2.84	2.84	2.64	1.74	0.77	3.95	1.74	1.42	1.30	1.30	1.30	1.30	1.42	1.74	3.88
$CHCl_3$-eluted part[a]	6.91	7.45	7.37	7.05	7.01	6.78	2.84	2.84	2.67	1.74	0.73	3.95	1.74	1.44	1.31	1.31	1.31	1.31	1.44	1.74	3.90
linear[b] (M_n = 12 700)	6.92	7.46	7.37	7.05	7.01	6.79	2.84	2.84	2.67	1.75	0.74	3.96	1.75	1.44	1.32	1.32	1.32	1.32	1.44	1.75	3.90
$\Delta\delta$[c]	0.01	0.10	0.23	0.37	0.37	0.25	−0.29	0.40	0.05	−0.08	−0.18	−0.22	0.09	0.07	0.25	0.25	0.25	0.25	0.20	0.21	0.08

[a] There are also minor peaks which are assigned to terminal groups (t1, 5.79 ppm, CH=CH_2; t2, 4.95 ppm, CH=CH_2; t3, 3.63 ppm, CH_2OH). [b] There are also minor peaks which are assigned to terminal groups (5.79 ppm, CH=CH_2; 4.95 ppm, CH=CH_2; 3.39 ppm, CH_2Br). [c] $\Delta\delta$ is the chemical shift difference between cyclic monomer and linear polyether ($\delta_{\text{linear polymer}} - \delta_{\text{cyclic monomer}}$).

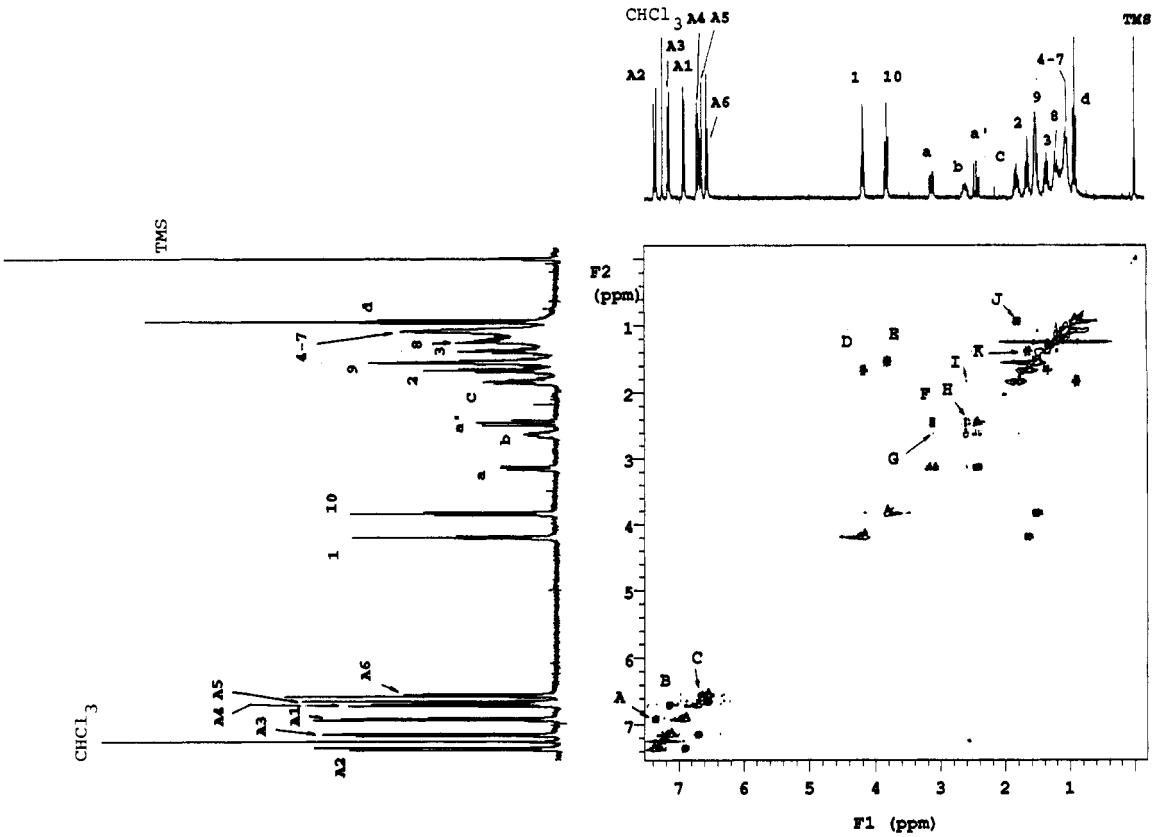

Figure 7. 2-D ^{1}H-NMR COSY spectrum of the cyclic monomer ($CDCl_3$, TMS).

of cyclic pentamer. The cyclic pentamer has a relatively broad transition peak and represents a mixture of pentamer with trimer, tetramer, and higher cyclic oligomers. Its purity could not be estimated due to the severe overlapping of all compounds. The calculated and measured molecular weights of the cyclic oligomers are plotted versus the ring size in Figure 5. The measured molecular weight is proportional to the ring size and is higher than the calculated value. This linear dependence is considered to be proof of the correct assignment of the ring size. The higher measured value compared to the calculated one suggests a larger hydrodynamic volume of the cyclic oligomers than that of the linear polystyrene in chloroform due to the presence of the semirigid mesogenic unit.

Characterization of Cyclic Oligomers by NMR Spectroscopy. Figure 6a–f presents the 300-MHz ^{1}H-NMR spectra of cyclic monomer, cyclic dimer, cyclic trimer, cyclic tetramer, cyclic pentamer, and the high molecular weight part eluted with chloroform. The ^{1}H-NMR spectrum of the low molecular weight linear polyether (M_n = 12 700) is identical to the spectrum 6f except for the structure of the chain ends (Table II), which will be discussed in more detail later. Figure 7 presents the 300-MHz 2-D ^{1}H-NMR COSY spectrum of the cyclic monomer, while Figure 8 presents the 300-MHz 2-D ^{1}H-NMR NOESY spectra of the cyclic monomer. The complete peak assignment of the NMR spectra was accomplished by using the COSY and NOESY 2-D ^{1}H-NMR techniques. COSY and NOESY spectra provide us with the information about the presence of through-bond coupling and through-space interactions, respectively. Both spectra contain diagonal peaks corresponding to the shifts in the normal ^{1}H-NMR spectra; off-diagonal peaks at the intersection of two chemical shifts indicate coupling two protons in the COSY spectrum or the proximity (<5 Å) of two protons if present in the NOESY spectrum. An example of the peak assignment process is demonstrated with COSY and NOESY spectra of cyclic monomer as follows.

The interpretation of the COSY spectrum of the cyclic monomer shown in Figure 7 started with the aromatic region. This area exhibits three crosspeaks which corre-

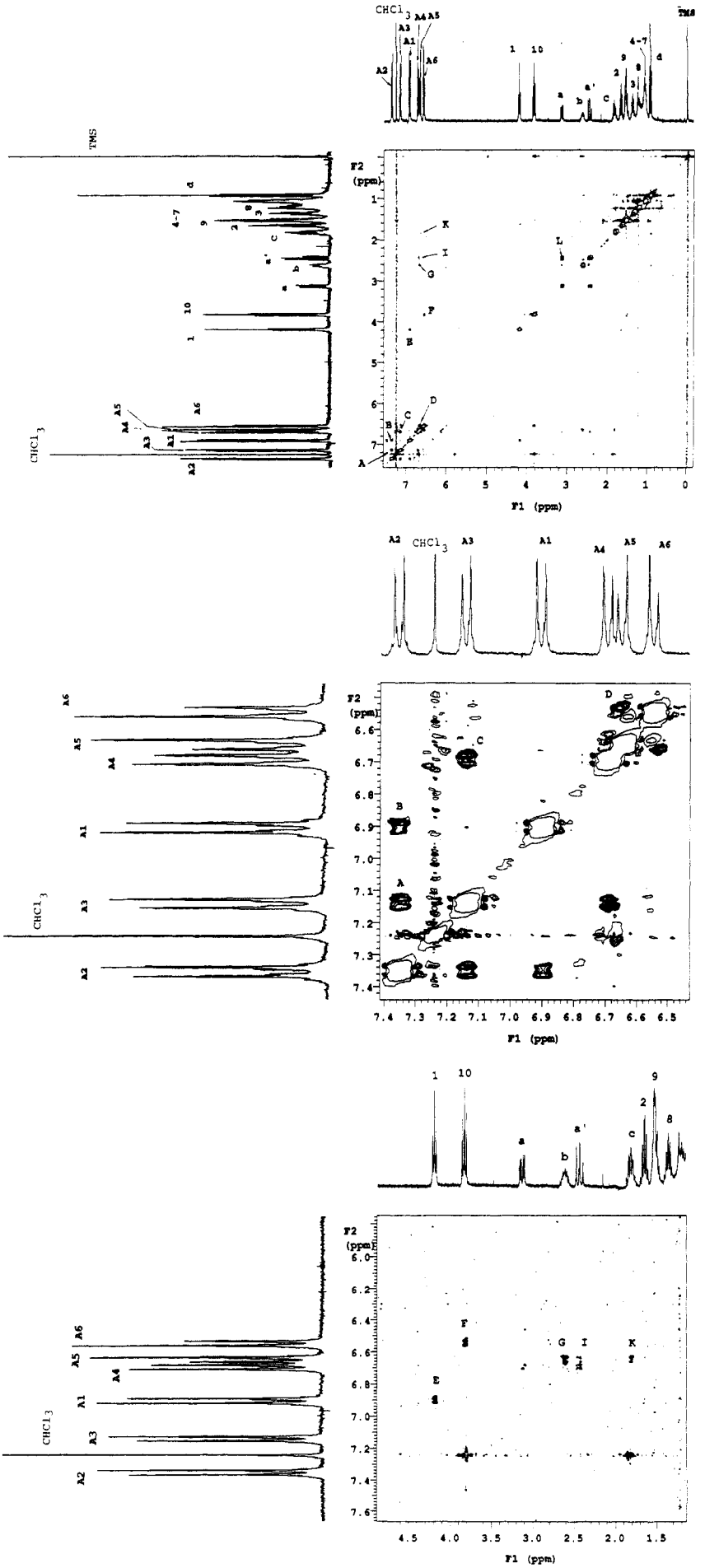

Figure 8. 2-D ^{1}H-NMR NOESY spectrum of the cyclic monomer ($CDCl_3$, TMS): (a, top) full scale; (b, middle) aromatic region (expansion); (c, bottom) aromatic–aliphatic region (expansion).

spond to the presence of through-bond couplings. Crosspeak A correlates peaks A1 and A2. Crosspeak B correlates peaks A3 and A4, while crosspeak C correlates peaks A5 and A6. Therefore, the protons corresponding to the A1 and A2 peaks, the protons corresponding to the A3 and A4 peaks, and the protons corresponding to the A5 and A6 peaks should be on the same phenyl ring, respectively. In the aliphatic region, crosspeak D shows the correlation between peaks 1 and 2, while crosspeak E shows the correlation for peaks 10 and 9. The methylene protons next to the aromatic ether usually show up around 4 ppm. Therefore, peaks 1 and 10 can be assigned to these protons, and the protons corresponding to peaks 2 and 9 should be from the methylenes next to these protons. Crosspeak F correlates peaks a and a′. Crosspeak G shows correlation between peaks a and b. Crosspeak H shows through-bond coupling for peaks a′ and b. Crosspeak I shows correlation between peaks b and c, while crosspeak J shows correlation between peaks c and d. Peak d is apparently due to the protons of the methyl group. Therefore, peak c can be assigned to the methylene protons next to the methyl group. From the correlation between peaks b and c, peak b is assigned to the methine proton next to the monophenyl ring, while a and a′ are assigned to the methylene protons next to the biphenyl ring. Peaks 2 and 3 are correlated by crosspeak K. Therefore, the protons corresponding to peak 3 should be next to the protons corresponding to peak 2.

Interpretation of the NOESY spectrum of the cyclic monomer started with the aromatic region (Figure 8b). Crosspeak A shows the proximity of protons responsible for peaks A2 and A3, crosspeak B correlates peaks A2 and A1, crosspeak C correlates peaks A3 and A4, and crosspeak D correlates peaks A5 and A6. However, the protons corresponding to peaks A2 and A3 are not on the same ring as discussed in the COSY spectrum. Therefore, it is possible to assign these protons to the biphenyl protons ortho to the phenyl rings. There are also crosspeaks correlating the aromatic and the aliphatic regions. Crosspeak E correlates peaks A1 and 1 while crosspeak F correlates peaks A6 and 10, indicating that the protons producing peaks A1 and A6 should be ortho to the ether linkages. This provides enough information about the relative positions of the aromatic protons. Thus A1 is due to the protons ortho to the ether group on the biphenyl ring, while A2 is due to the protons ortho to the ether group on the same ring. A3 is due to the protons meta to the methylene group on the biphenyl ring, while A4 is due to the protons ortho to the methylene group on the same ring. Furthermore, A5 is due to the protons meta to the ether group on the monophenyl ring, while A6 is due to the protons ortho to the ether group on the same ring. There are other crosspeaks correlating the aromatic and the aliphatic regions: crosspeak G shows the correlation between peaks A5 and b, and crosspeak I correlates peaks A4 and a′. Therefore, peak a′ should be assigned to one of the protons of the methylene group next to the biphenyl ring, and peak b should be assigned to the methine proton. These assignments are consistent with those made from the COSY spectrum. Crosspeak K shows the correlation between peaks A5 and c, which was assigned to methylene protons next to the methyl group. In the aliphatic region there is crosspeak L, correlating peaks a and a′. The assignments of the proton resonances of the other cyclics were accomplished by the same process with both COSY and NOESY spectra.

The assignments of all peaks are summarized in Table II and Scheme II. The patterns of the ^{1}H-NMR spectra

Scheme II
^{1}H-NMR Peak Assignments of Cyclic Oligomers

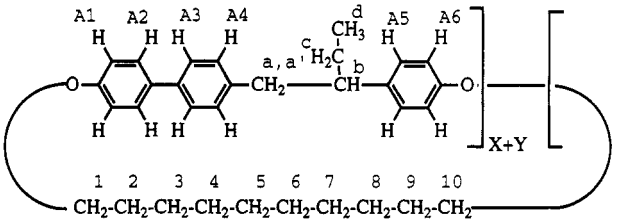

X+Y= Ring Size

change dramatically as the size of the macrocyclic ring increases from monomer to pentamer. Figure 9a presents the chemical shifts of aromatic protons (A1–A6) versus ring size. Most of the protons shift to a lower field with increasing ring size except the protons (A1) ortho to the ether group on the biphenyl ring, whose chemical shift does not change with the ring size. The differences between the chemical shifts of various protons of the cyclic monomer and the linear polymer are summarized as $\Delta\delta$ in Table II. As the positions of the protons on the phenyl rings move further from the ethylene unit connecting the monophenyl ring and the biphenyl ring, $\Delta\delta$ becomes smaller. This behavior can be explained as follows. Figure 10 presents the lowest free energy conformation of the cyclic monomer. In the cyclic monomer TPB is considered to primarily adopt a gauche conformation due to the restricted length of the spacer. In this conformation the monophenyl ring and the phenyl ring next to the methylene group of the biphenyl ring become close to each other and shield the protons of each phenyl ring. This shielding effect shifts them upfield. However, the A1 protons are too far away to be affected by the monophenyl ring. The A2 protons have a relatively smaller effect. In the case of the dimer the anti conformation becomes possible. However, it should still adopt a gauche conformation to some extent since both conformers are in dynamic equilibrium. As the ring size becomes larger, the anti conformation of the mesogen becomes more favorable, and the chemical shifts move to lower field as the protons experience the environment of the anti conformation for a larger fraction of time. On the other hand, the methyl protons (d) and the methylene protons (c) of the ethyl group of the mesogenic unit shift to higher field with increasing ring size as presented in Figure 9b since the anti conformation places these protons over the shielding regions of the phenyl rings for a large fraction of time. The chemical shifts of the methylene protons (a and a′) next to the biphenyl ring also change dramatically as shown in Figure 9c. These protons are diastereomeric protons since they are next to the chiral center. Therefore, these protons have a different chemical shift in the cyclic oligomers. These become closer with increasing ring size and become a simple doublet in the linear polymer. This phenomenon can also be explained by the dynamic conformational change between the gauche and anti conformers and their ratio. The chemical shift of the methine proton (b) is not affected by the ring size. The chemical shift of the methylene protons (1–10) in the spacer shifts differently depending on position, as presented in Figure 9d. The methylene protons next to the biphenylyloxy group shift to higher field with increasing ring size, while the other protons shift to lower field. This can be explained as follows: in the cyclic monomer the methylene protons next to the biphenyl ring are aside of the phenyl ring while the other methylene protons are placed mostly above the biphenyl ring.

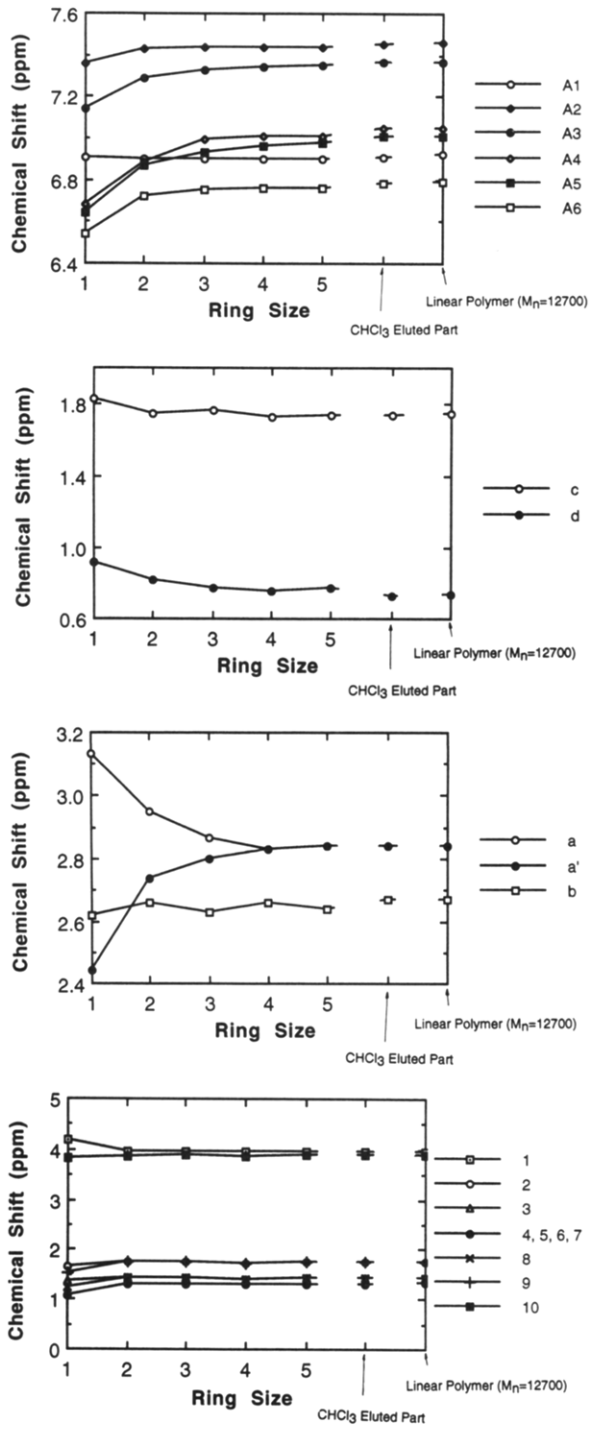

Figure 9. Dependence of chemical shifts on ring size: (a, top) aromatic protons (A1–A6); (b, upper middle) protons of the lateral ethyl group (c and d); (c, lower middle) methylene protons next to the biphenyl ring (a and a′) and methine proton (b); (d) methylene protons in the spacer (1–10).

These NMR results demonstrate that the semiflexibility of the TPB mesogenic unit contributes to the formation of cyclic oligomers and polymers.

Two kinds of terminal groups (t1, t2, t3), i.e., CH_2OH, and $CH{=}CH_2$, were detected in the ^{1}H-NMR spectrum of the high molecular weight part eluted with chloroform (Figure 6f, Table II). Terminal CH_2Br and $CH{=}CH_2$ were also detected in the ^{1}H-NMR spectrum of the linear polymer with almost the same molecular weight (Table II). The number of terminal groups in the high molecular weight part which eluted with chloroform was estimated from the ^{1}H-NMR spectrum to be about half that of the linear polymer (M_n = 12 700). Consequently, the chloroform-eluted fraction contains 50 mol % of the larger cyclic polyethers. The vinyl groups originate from the elimination of HBr from the bromide chain ends of the spacer, while the alcohol groups are produced by the hydrolysis of the bromide groups.

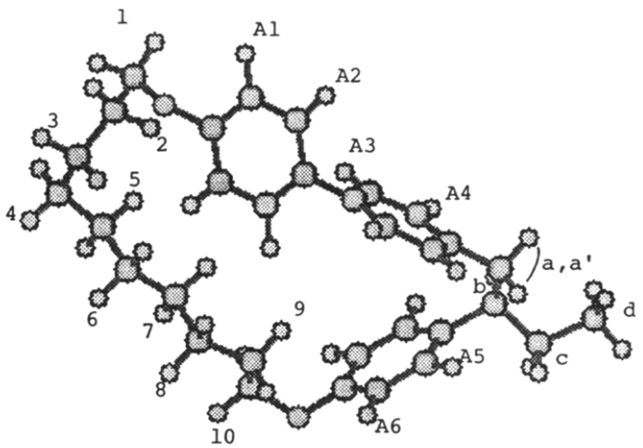

Figure 10. Lowest free energy conformation of the cyclic monomer.

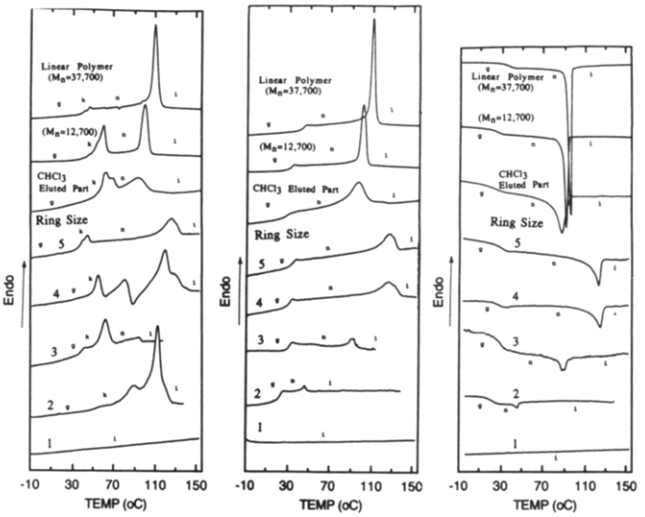

Figure 11. DSC thermograms of the linear polyethers, of the part eluted with $CHCl_3$, and of the cyclic oligomers: (a, left) first heating scans; (b, middle) second heating scans; (c, right) first cooling scans.

Phase Behavior of Cyclic Oligomers. Figure 11a presents the first heating DSC scan while Figure 11b,c presents the second heating and first cooling DSC scans of the cyclic oligomers and linear polymers. The thermal transition temperatures and the corresponding enthalpy changes collected from first heating, second heating, and first cooling scans are summarized in Table I. The cyclic monomer, which at room temperature is a liquid, does not show any phase transition between −10 and +155 °C. The cyclic dimer exhibits a glass transition temperature (T_g) and melting transitions during the first heating scan. An isotropic–nematic transition, a nematic–isotropic transition, and T_g are observed during the cooling and second heating scans of the cyclic dimer. Figure 12a illustrates the schlieren nematic texture of the cyclic dimer obtained after annealing at 42.3 °C for 14 min followed by cooling from the isotropic phase. T_m observed in the first heating scan of the cyclic dimer is higher than T_{ni} observed during the second heating scan. Actually, upon heating above T_{ni} the crystallization of the sample started around 60 °C as observed on the optical polarized micrograph presented in Figure 12b. After annealing at 85.9 °C for 5 min, the

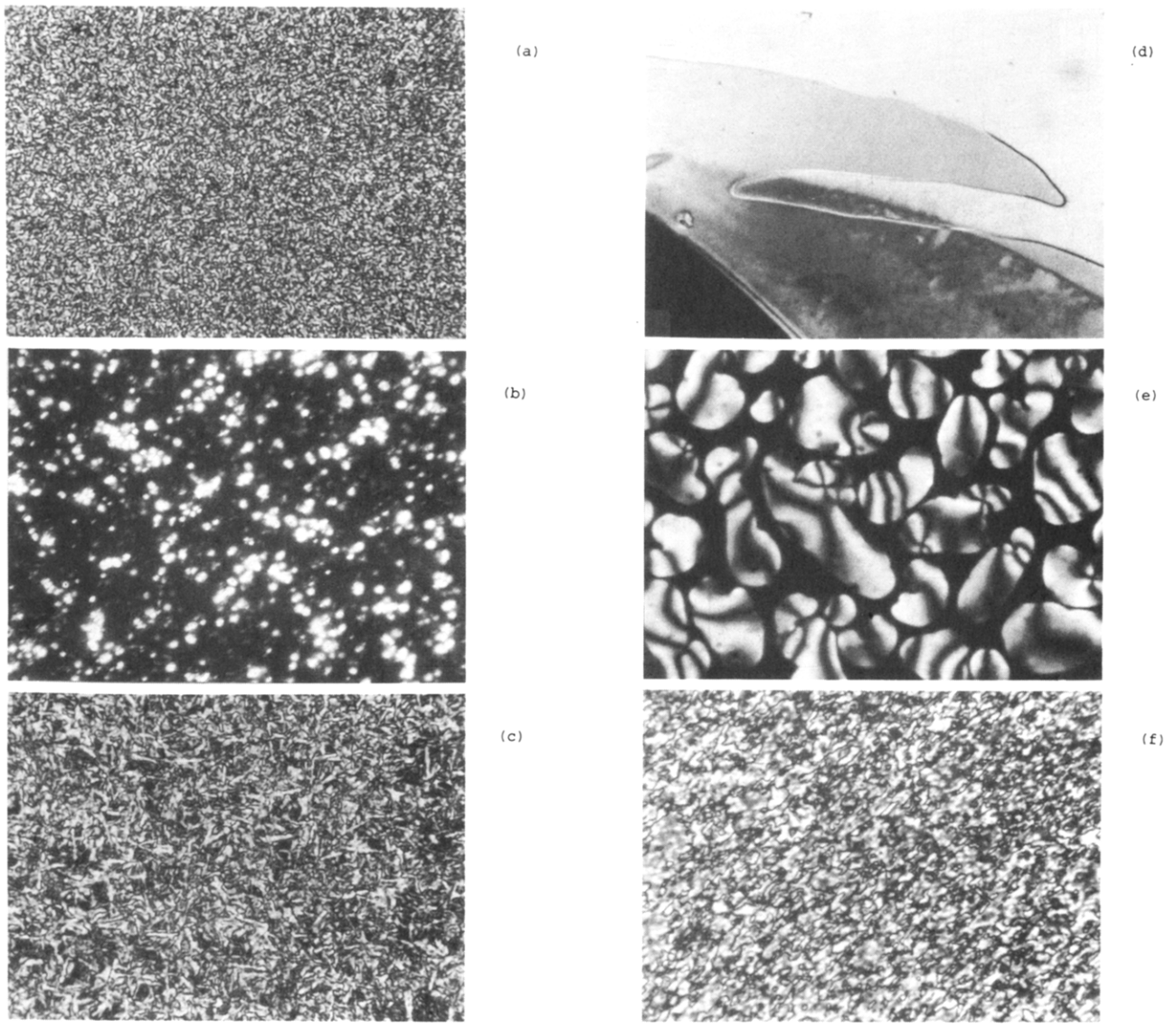

Figure 12. Textures of the cyclic oligomers observed under the optical polarized microscope (original magnification ×300; the micrographs have been reduced to 55% of their original size for publication purposes): (a) cyclic dimer after anealing at 42.3 °C for 14 min; (b) cyclic dimer upon heating from (a) at 60.1 °C; (c) cyclic dimer after anealing at 85.9 °C for 5 min; (d) cyclic trimer after anealing at 79.8 °C for 13 min; (e) cyclic tetramer after anealing at 113.4 °C for 3 min; (f) cyclic tetramer upon cooling from (a) at 56.5 °C (after shearing).

needlelike crystalline texture was observed as presented in Figure 12c. Therefore, under equilibrium conditions the nematic mesophase of the dimer is considered to be monotropic.

The cyclic trimer shows T_g, melting, and an enantiotropic nematic mesophase during the first heating scan. However, only the isotropic–nematic transition, nematic–isotropic transition, and T_g are observed during the cooling and second heating scans of the cyclic trimer. Figure 12d presents the nematic texture of the cyclic trimer obtained after annealing at 79.8 °C for 13 min.

The cyclic tetramer shows a complicated DSC thermogram during its first heating scan. After T_g, two melting followed by crystallization and a melting into a nematic phase followed by isotropization transitions are observed. However, only an isotropic–nematic transition, a nematic–isotropic transition, and T_g are observed during the cooling and second heating scans. Figure 12e presents the texture of the nematic phase of the cyclic tetramer obtained after annealing at 113.4 °C for 3 min.

The crude cyclic pentamer also exhibits T_g, melting, and nematic–isotropic transitions during the first heating scan. Only an isotropic–nematic transition, a nematic–isotropic transition, and T_g are observed during the cooling and second heating scans.

As a general comment we can state that all cyclic oligomers have a very low tendency toward crystallization. The resulting transition temperatures of the cyclic compounds exhibit a strong odd–even dependence on ring size. However, the isotropization transition temperature of the cyclic compounds shows a steady increase with ring size. This result might be due to the presence of a single structure of the cyclic molecule in the crystalline phase, while in the nematic phase there is a dynamic equilibrium between its various structures. A speculative explanation for the odd–even effect of the melting temperature is as follows. The cyclics with an even degree of polymerization, i.e., the dimer and the tetramer, can pack in a crystalline phase containing only the anti conformer of the mesogen, while the cyclics with an odd degree of polymerization, i.e., the trimer and the pentamer, require both the anti and gauche conformers of the mesogen in their structure. This last situation may generate a crystalline phase with a lower degree of order (Figure 13). Therefore, the cyclics with an even degree of polymerization may have a lower entropy in the crystalline phase

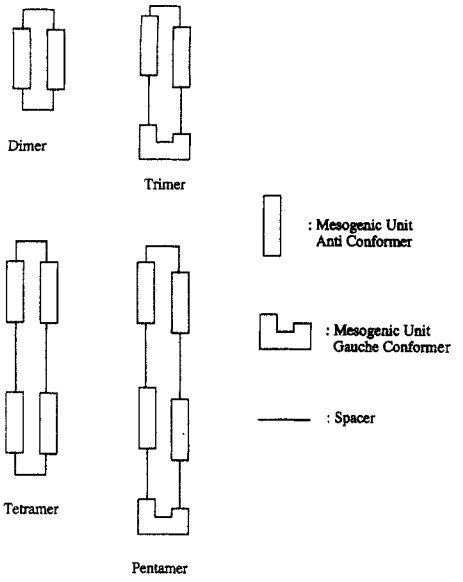

Figure 13. Possible molecular arrangement of cyclic oligomers in the crystalline phase.

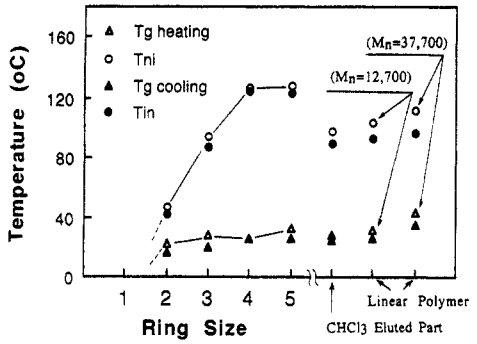

Figure 14. Transition temperatures of the cyclic oligomers obtained during second heating and first cooling scans versus the ring size and comparison with their linear homologues.

and a higher melting temperature than the cyclics with an odd degree of polymerization do. Elucidation of the crystalline structure of these cyclics is nevertheless required to confirm this speculative explanation.

The chloroform-eluted part represents a mixture of larger cyclics and linear polymers and shows T_g, melting, and nematic–isotropic transitions during the first heating scan. Only an isotropic–nematic transition, a nematic–isotropic transition, and T_g are observed during the cooling and second heating scans. The peaks of the nematic–isotropic transitions are relatively broad. In this case the polymer is acutally a mixture of both linear and cyclic polymers which may have different isotropization transition temperatures, and, therefore, this mixture broadens the isotropization transition peaks.

Figure 14 presents the transition temperatures collected during the second heating and cooling scans vs the ring size. T_g increases slightly as the ring size increases while T_{ni} and T_{in} increase rapidly with the increase of the ring size. However, T_{ni} of the $CHCl_3$-eluted part, which is a mixture of linear and cyclic polyethers, is lower than that of the cyclic tetramer and pentamer. Also the T_{ni} of the tetramer and crude pentamer are higher than even that of the linear TPB-10 with M_n = 37 700.[13] The entropy change associated with the nematic–isotropic transition during the second heating and cooling scans tends to increase with increasing ring size as presented in Figure 15. Another interesting behavior of the cyclic compounds is found in their isotropization peaks. Although the cyclic compounds are monodisperse products their isotropization peaks are broader than those of the linear high molecular weight polymer (Figure 11b,c).[13]

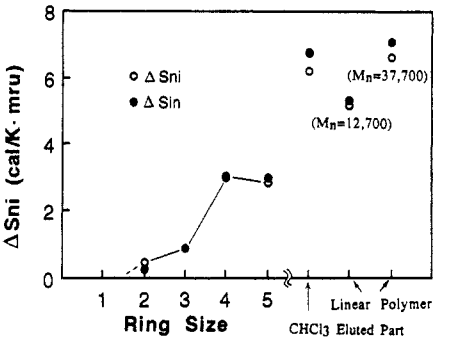

Figure 15. Entropy change associated with the nematic–isotropic transitions of the cyclic oligomers obtained during second heating and first cooling scans versus ring size and comparison with their linear homologues.

Scheme III
Schematic Representation of the Isotropic–Nematic Transition of the Cyclic Tetramer

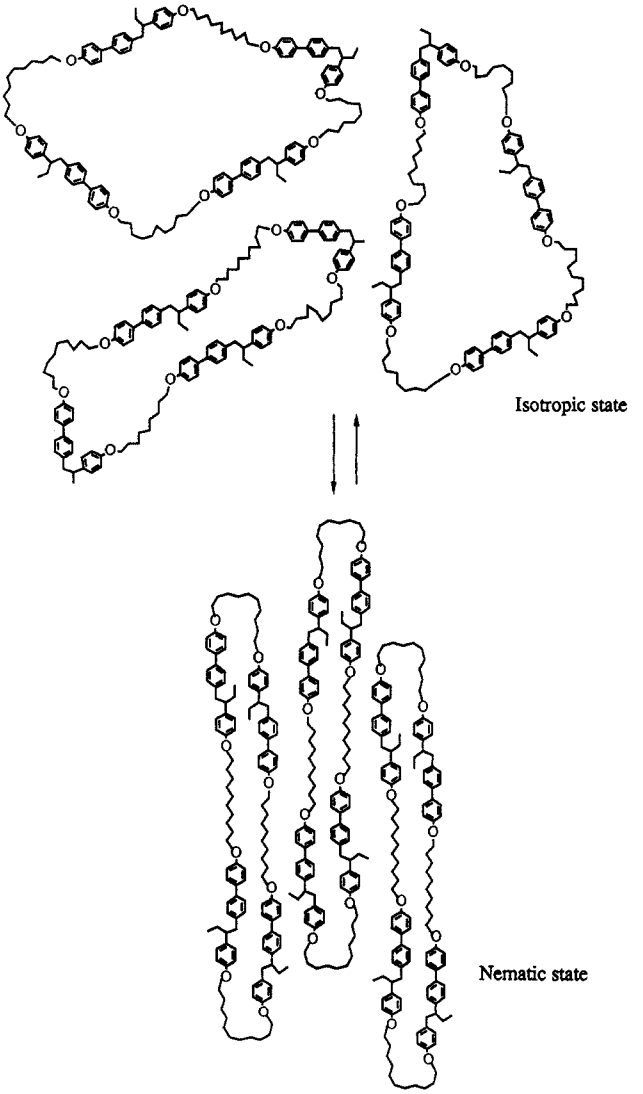

Scheme III outlines the isotropic–nematic transition of the cyclic tetramer as an example. As observed from Scheme III, due to the molecular recognition of the mesogenic groups, these cyclics have a distorted conformation, which is required to explain their liquid crystallinity. They resemble the cyclic oligomers of polyethylene.[9] While linear compounds exhibiting nematic mesophases show translational and rotational motions, cyclic liquid crystals

provide most probably the translational motion of their mesogenic group mostly via a jump reptation motion which changes the conformation of the mesogen and spacer when they pass through the fold. In linear oligomers and polymers the middle spacers are extended while their chain ends are melted. In cyclics there are no chain ends, and, although in the fold there are both cis and trans conformations of the groups of methylene units, they are rigid. Simultaneously, the cyclic structure has a lower entropy in the isotropic phase than that of the corresponding linear oligomer. The entropy change of isotropization of the cyclic oligomers varies from 1 to 3 cal/(mru K), while that of the high molecular weight linear polymers varies from 5 to 7 cal/(mru K) (Table I). Therefore, the difference in entropy between the isotropic and nematic phase of cyclics is lower than that of linear compounds. At the same time since the chain ends (i.e., the fold) of cyclics are rigid, they can explain their higher isotropization transition temperatures versus those of the corresponding linear oligomers with similar molecular weights. Nevertheless, the difference between the ridigity of the chain ends of cyclic oligomers and high molecular weight linear polymer cannot explain the difference between their isotropization transition temperatures. Therefore, we can assume that the overall ridigity of the cyclic oligomers is higher than that of the high molecular weight linear polymers. Finally, the jump reptation mechanism can explain the broad isotropization peaks of the cyclic compounds. Although they are individual molecules, the conformational change of the mesogen and spacer when they pass through the fold makes them behave as mixtures of different compounds which are present in a dynamic equilibrium.

Although numerous experiments are still required to eludicate the mesomorphic behavior of cyclic oligomers and polymers versus that of linear oligomers and polymers, the experiments described here are nevertheless providing numerous new synthetic opportunities for polymers based on cyclic mesogenic structural units.

Acknowledgment. Financial support by the National Science Foundation, Polymers Program (Grant DMR-86-19724), and Toyota Central Research & Development Laboratories, Nagoya, Japan, is gratefully acknowledged.

References and Notes

(1) This paper is Part 24 in the series "Liquid Crystalline Polyethers Based on Conformational Isomerism". Part 23: Percec, V.; Kawasumi, M. *Macromolecules*, preceding paper in this issue.

(2) (a) Percec, V.; Pugh, C.; Nuyken, O.; Pask, S. D. In *Comprehensive Polymer Science*; Allen, G., Bevington, J. C., Eds.; Pergamon Press: Oxford, 1989; Vol. 6, p 281. (b) Rempp, P.; Strazielle, C.; Lutz, P. In *Encyclopedia of Polymer Science and Engineering*, 2nd ed.; Mark, H. F., Bikales, N. M., Overberger, C. G., Menges, G., Kroschwitz, J. I., Eds.; Wiley: New York, 1987, Vol. 9, p 183. (c) Semlyen, J. A., Ed. *Cyclic Polymers*; Elsevier Applied Science Publishers: New York, 1986.

(3) Hilgenfeld, R.; Saenger, W. *Top. Curr. Chem.* **1982**, *101*, 1.

(4) (a) Vollmert, B.; Huang, J. X. *Makromol. Chem., Rapid Commun.* **1981**, *2*, 467. (b) Geiser, D.; Höcker, H. *Macromolecules* **1980**, *13*, 653. (c) Roovers, J.; Toporowski, P. *Macromolecules* **1983**, *16*, 843. (d) Roovers, J. *Macromolecules* **1985**, *18*, 1359. (e) Hild, G.; Kohler, A.; Rempp, P. *Eur. Polym. J.* **1980**, *16*, 525. (f) Hild, G.; Kohler, A.; Rempp, P. *Eur. Polym. J.* **1983**, *19*, 721. (g) Sundararajan, J.; Hogen-Esch, T. E. *Polym. Prepr. (Am. Chem. Soc., Div. Polym. Chem.)* **1991**, *32* (3), 604.

(5) (a) Clarson, S. J.; Semlyen, J. A. *Polymer* **1986**, *27*, 1633. (b) Clarson, S. J.; Dodgson, K.; Semlyen, J. A. *Polymer* **1985**, *26*, 930. (c) Kuo, C. M.; Clarson, S. J. *Polym. Prepr. (Am. Chem. Soc., Div. Polym. Chem.)* **1991**, *32* (3), 595.

(6) Sundararajan, J.; Hogen-Esch, T. E. *Polym. Prepr. (Am. Chem. Soc., Div. Polym. Chem.)* **1991**, *32* (1), 63.

(7) (a) Brunelle, D. J.; Evance, T. L.; Shannon, T. G.; Boden, E. P.; Stewart, K. R.; Fontana, L. P.; Bonauto, D. K. *Polym. Prepr. (Am. Chem. Soc., Div. Polym. Chem.)* **1989**, *30* (2), 569. (b) Brunelle, D. J.; Boden, E. P.; Shannon, T. G. *J. Am. Chem. Soc.* **1990**, *112*, 2399.

(8) (a) Colquhoun, H. M.; Dudman, C. C.; Thomas, M.; O'Mahoney, C. A.; Williams, D. J. *J. Chem. Soc., Chem. Commun.* **1990**, 336. (b) Buese, M. A. *Macromolecules* **1990**, *23*, 4341.

(9) Möller, M.; Waldron, R. F.; Drotloff, H.; Emeis, D. *Polymer* **1987**, *28*, 1200.

(10) (a) Percec, V.; Hahn, B. *J. Polym. Sci., Polym. Chem. Ed.* **1989**, *27*, 2367. (b) Richards, R. D. C.; Hawthorne, W. D.; Hill, J. S.; White, M. S.; Lacey, D.; Semlyen, J. A.; Gray, G. W.; Kendrick, T. C. *J. Chem. Soc., Chem. Commun.* **1990**, 95.

(11) Percec, V.; Yourd, R. *Macromolecules* **1989**, *22*, 524, 3229.

(12) Percec, V.; Tsuda, Y. *Macromolecules* **1990**, *23*, 3520.

(13) Percec, V.; Kawasumi, M. *Macromolecules* **1991**, *24*, 6318.

(14) Diedrich, F. *Cyclophanes, Monographs in Supramolecular Chemistry Series*; Stoddart, J. F., Ed.; Royal Society of Chemistry: Cambridge, 1991.

(15) (a) Demus, D.; Richter, L. *Textures of Liquid Crystals*; Verlag Chemie: Weinheim, 1978. (b) Gray, G. W.; Goodby, J. W. *Smectic Liquid Crystals. Textures and Structures*; Heyden and Son Inc.: Philadelphia, 1984.

Registry No. TPB/Br$(CH_2)_{10}$Br (copolymer), 136089-71-9; TPB/Br$(CH_2)_{10}$Br (cyclic monomer), 141848-31-9; TPB/Br$(CH_2)_{10}$Br (cyclic dimer), 141848-32-0; TPB/Br$(CH_2)_{10}$Br (cyclic trimer), 141879-12-1; TPB/Br$(CH_2)_{10}$Br (cyclic tetramer), 141848-33-1; TPB/Br$(CH_2)_{10}$Br (cyclic pentamer), 141848-34-2.